

On the Information Loss of the Max-Log Approximation in BICM Systems

Mikhail Ivanov, Christian Häger, Fredrik Brännström, Alexandre Graell i Amat, Alex Alvarado, and Erik Agrell

Abstract—We study different aspects of achievable information rates for a bit-interleaved coded modulation (BICM) system. It is commonly assumed that the calculation of L-values using the max-log approximation leads to an information loss. We show that this is not always true. For symmetric 4-ary pulse-amplitude modulation (PAM) constellations labeled with a Gray code, we prove that the max-log approximation does not cause any information loss, while for all other combinations of PAM constellations and labelings, this approximation is indeed lossy. We also show that for max-log L-values, the BICM generalized mutual information (GMI), which is an achievable rate for a standard BICM decoder, is too pessimistic. In particular, we prove that the so-called “harmonized” GMI, which can be seen as the sum of bit-level GMIs, is achievable without any modifications to the decoder. We then study how bit-level channel symmetrization and mixing affect the mutual information (MI) and the GMI for max-log L-values. Our results show that these operations, which are often used when analyzing BICM systems, do not change the GMI. However, when the max-log approximation is lossy, these operations reduce the MI.

I. INTRODUCTION

Bit-interleaved coded modulation (BICM) [1] is a pragmatic approach to achieve high spectral efficiency with binary error-correcting codes. Because of its inherent simplicity and flexibility, as well as good performance, it is implemented in many practical wireless communication systems [2]–[4].

A central part of a BICM system is the demapper, which computes soft information about the coded bits in the form of so-called L-values. Ideally, L-values correspond to log-likelihood ratios, in which case we refer to them as exact L-values. In practice, however, the demapper often only computes approximate L-values due to complexity reasons. A common approximation is to replace the log-sum operation in the log-likelihood ratio computation with a max-log operation. This approximation can be motivated by the fact that at high signal-to-noise ratio (SNR), exact and approximate max-log L-values are almost identical.

In this paper, we analyze achievable rates of BICM for symmetric nonbinary pulse-amplitude modulation (PAM) con-

stellations over the additive white Gaussian noise (AWGN) channel, paying special attention to max-log L-values. Traditionally, achievable rates for BICM systems are analyzed for exact L-values under the assumption of an ideal interleaver [5], which results in the BICM mutual information (MI) (i.e., the sum of m bit-level MIs), often referred to as the BICM capacity. In [6], it was proposed to analyze BICM from a mismatched decoding perspective, showing that the maximum achievable rate for a BICM system is lowerbounded by the BICM generalized mutual information (GMI), without invoking any interleaver assumption. For exact L-values, the BICM GMI coincides with the BICM MI [6].

When max-log L-values are considered, most of the previous work concentrates on the correction of the “suboptimal” L-values in order to either maximize the BICM GMI [7], [8] or minimize the error probability [9]. To the best of our knowledge, a rigorous comparison of achievable rates in terms of the BICM MI and the BICM GMI for max-log L-values has not yet been carried out. Despite this fact, it seems to be a common belief in the literature that the calculation of max-log L-values is inherently an information lossy operation. As an example, when discussing the MI between the transmitted information symbol and the vector of max-log L-values at the output of the demapper, [10, p. 137] concludes that “the approximation clearly constitutes a lossy procedure and entails an inferior BICM capacity”. Similar implicit assumptions are made in [11] and [12]. The main contribution of this paper is to show that this conclusion is not always true. In particular, we prove that for symmetric 4-PAM constellations labeled with the binary reflected Gray code (BRGC), no information loss occurs when comparing exact and max-log L-values, i.e., the BICM MI is the same in both cases. We also prove that for all other combinations of PAM constellations and labelings, the max-log approximation indeed induces an information loss.

We then study the BICM GMI for max-log L-values. In particular, the so-called “harmonized” GMI was introduced in [8] as an achievable rate for a modified BICM decoder that applies scaling factors to the L-values. In this paper, we argue that the L-value scaling is in fact unnecessary, and the harmonized GMI (which can be seen as the sum of m bit-level GMIs) is achievable without any modifications to the decoder. Finally, we analyze two common processing techniques which are often used in the theoretical analysis of BICM systems: bit-level channel symmetrization and channel mixing. The results show that these operations do not affect the BICM GMI but can reduce the BICM MI.

This research was supported by the Swedish Research Council, Sweden, under Grant No. 2011-5950, in part by the Ericsson’s Research Foundation, Sweden, under Grant No. 556016-0680, and in part by the European Community’s Seventh’s Framework Programme (FP7/2007-2013) under grant agreement No. 271986. The calculations were performed on resources provided by the Swedish National Infrastructure for Computing (SNIC) at C3SE.

M. Ivanov, C. Häger, F. Brännström, A. Graell i Amat, and E. Agrell are with the Dept. of Signals and Systems, Chalmers Univ. of Technology, SE-41296 Gothenburg, Sweden (e-mail: {mikhail.ivanov, christian.haeger, fredrik.brannstrom, alexandre.graell, agrell}@chalmers.se).

A. Alvarado is with the Optical Networks Group, Dept. of Electronic & Electrical Engineering, Univ. College London, WC1E 7JE London, UK (e-mail: alex.alvarado@ieee.org).

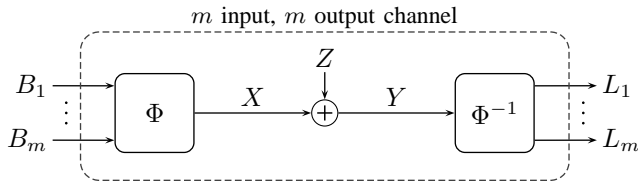


Fig. 1: Block diagram of the analyzed system.

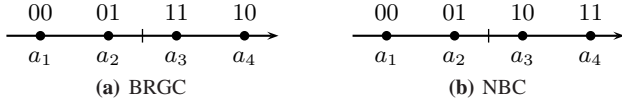


Fig. 2: Equally spaced 4-PAM constellation with two different binary labelings.

A. Notation

Throughout the paper, boldface letters \mathbf{x} denote row vectors, blackboard letters \mathbb{X} denote matrices, and capital letters X denote random variables. $\mathbf{1}_n$ and $\mathbf{0}_n$ denote all-one and all-zero vectors of length n , respectively. Calligraphic letters \mathcal{X} denote sets, where \mathbb{R} stands for the set of real numbers. We define $\mathcal{B} = \{0, 1\}$. If $b \in \mathcal{B}$, then $\check{b} = (-1)^b \in \{-1, +1\}$ and $\bar{b} = 1 - b$. $\mathbb{E}\{\cdot\}$ denotes expectation and $\Pr\{\cdot\}$ represents probability. The probability density function (PDF) of a continuous random variable Y is denoted by $f_Y(\cdot)$ and the conditional PDF by $f_{Y|X}(\cdot|\cdot)$.

II. SYSTEM MODEL

A block diagram of the considered system model, which we discuss in the following, is shown in Fig. 1.

A. Modulator

A modulator Φ is fed with m bits B_j , $1 \leq j \leq m$, and maps them to one of $M = 2^m$ possible constellation points. We consider symmetric PAM constellations denoted by $\mathcal{S} = \{a_1, \dots, a_M\}$, where $a_k < a_{k+1}$, $1 \leq k \leq M-1$ and $a_k = -a_{M-k+1}$, $1 \leq k \leq M$. The bits are assumed to be distributed according to $\Pr\{B_j = u\} = 1/2, \forall j$ and $u \in \{0, 1\}$, and thus, the symbols are equiprobable, i.e., $\Pr\{X = a_k\} = 1/M, \forall k$.

The constellation is assumed to be normalized to unit average energy $\mathbb{E}\{X^2\} = (1/M) \sum_{k=1}^M a_k^2 = 1$. In practice, equally spaced constellations are most commonly used. In this paper, all theorems hold for symmetric PAM constellations, whereas all the numerical examples are presented for an equally spaced 4-PAM constellation $\mathcal{S} = \{\pm 3/\sqrt{5}, \pm 1/\sqrt{5}\}$.

The mapping $\Phi: \{0, 1\}^m \rightarrow \mathcal{S}$ is assumed to be one-to-one and is defined by a binary labeling. The binary labeling is specified by an $m \times M$ binary matrix \mathbb{L} , where the k th column of \mathbb{L} is the binary label of the constellation point a_k . As an example, in Fig. 2 we show an equally spaced 4-PAM constellation with the two labelings

$$\mathbb{L}_1 = \begin{bmatrix} 0 & 0 & 1 & 1 \\ 0 & 1 & 1 & 0 \end{bmatrix}, \quad \mathbb{L}_2 = \begin{bmatrix} 0 & 0 & 1 & 1 \\ 0 & 1 & 0 & 1 \end{bmatrix} \quad (1)$$

which are often referred to as the BRGC and the natural binary code (NBC) or set-partitioning labeling [13], respectively. Furthermore, we define $\mathcal{S}_{j,u} = \{a_k \in \mathcal{S} : \mathbb{L}_{k,j} = u, \forall k\}$ as

the subconstellation where all points are labeled with the bit u in the j th bit position. We emphasize that all results naturally generalize to two-dimensional product constellations of M -PAM, i.e., M^2 -ary quadrature amplitude modulation (QAM) labeled with a product labeling.

Certain quantities, such as the L-values we define below, depend only on the subconstellations $\mathcal{S}_{j,0}$ and $\mathcal{S}_{j,1}$, i.e., they depend only on the j th row in \mathbb{L} . We refer to the j th row of \mathbb{L} as a bit pattern, or simply pattern, which was shown in [14] to be a useful tool for analyzing binary labelings. A pattern is defined as a vector $\mathbf{p}_j = [p_1, \dots, p_M] \in \{0, 1\}^M$ with Hamming weight $M/2$. A labeling \mathbb{L} can then be represented by m patterns, each corresponding to one row of \mathbb{L} . We define two trivial operations that can be applied to a pattern. A *reflection* of \mathbf{p} is defined as $\mathbf{p}' = \text{refl}(\mathbf{p})$ with $p'_k = p_{M+1-k}$. An *inversion* of \mathbf{p} is defined as $\mathbf{p}' = \text{inv}(\mathbf{p})$ with $p'_k = \bar{p}_k$. A pattern \mathbf{p}' that is related to another pattern \mathbf{p} via inversions and/or reflections is said to be equivalent to \mathbf{p} . Analogously, labelings related by trivial operations (i.e., row permutations, inversion, and/or reflection of all patterns in the labeling) are said to be equivalent [15, Definition 6b]. For example, there exist eight labelings that are equivalent to the BRGC for 4-PAM shown in Fig. 2(a). Equivalent patterns and labelings behave similarly, e.g., they give the same uncoded bit error rate (BER) and achievable rates.

B. AWGN Channel

The constellation points are assumed to be transmitted over the discrete-time memoryless AWGN channel with output $Y = X + Z$, where the noise Z is a zero-mean Gaussian random variable with variance $\mathbb{E}\{Z^2\} = N_0/2$. The conditional PDF of the channel output given the channel input is

$$f_{Y|X}(y|x) = \sqrt{\frac{\rho}{\pi}} e^{-\rho(y-x)^2} \quad (2)$$

where $\rho = 1/N_0$ is the average SNR.

C. Demappers

Two demappers Φ^{-1} are considered at the receiver. The first one calculates *exact* L-values as the log-likelihood ratios

$$l_j^{\text{ex}}(y) = \log \frac{f_{Y|B_j}(y|1)}{f_{Y|B_j}(y|0)} = \log \frac{\sum_{x \in \mathcal{S}_{j,1}} e^{-\rho(y-x)^2}}{\sum_{x \in \mathcal{S}_{j,0}} e^{-\rho(y-x)^2}}. \quad (3)$$

The second demapper calculates *max-log* L-values using the max-log approximation as [16]

$$l_j^{\text{ml}}(y) = \rho \left[\min_{x \in \mathcal{S}_{j,0}} (y-x)^2 - \min_{x \in \mathcal{S}_{j,1}} (y-x)^2 \right]. \quad (4)$$

The observation Y is a random variable and thus, so are the L-values. To simplify the notation, we use $L_j = L_j^{\text{ex}} = l_j^{\text{ex}}(Y)$ when discussing exact L-values and $L_j = L_j^{\text{ml}} = l_j^{\text{ml}}(Y)$ when discussing max-log L-values. We further define the vector $\mathbf{L} = [L_1, \dots, L_m]$ and write \mathbf{L}^{ex} and \mathbf{L}^{ml} when discussing exact and max-log L-values, respectively.

In Fig. 3, we show the exact and max-log L-values (normalized by $4\rho/5$) as functions of the observation y for the

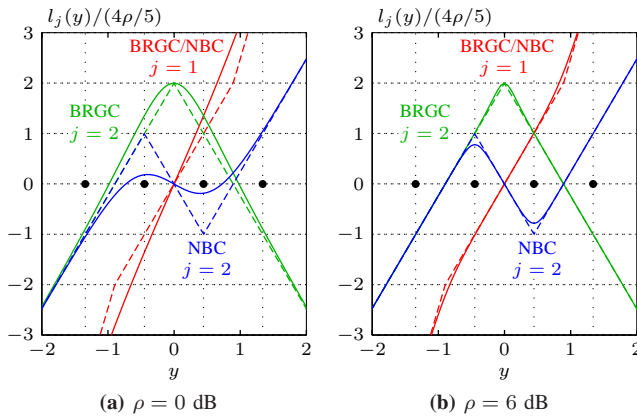


Fig. 3: Normalized exact (solid) and max-log (dashed) L-values as functions of the observation y assuming an equally spaced 4-PAM constellation labeled with the BRGC and NBC (see Fig. 2).

constellation and labelings shown in Fig. 2 and two different values of ρ . As shown in [11], the max-log L-value is a piecewise linear function of the observation, which simply scales with SNR, whereas the dependency of the exact L-value on the SNR is nonlinear. However, when the SNR increases, the exact L-value approaches the max-log L-value.

D. Coding Scheme

We consider a coding scheme where an information message is mapped to a codeword $\mathbf{x} = [x_1, \dots, x_N]$, $x_i \in \mathcal{S}$, $1 \leq i \leq N$, and N corresponds to the number of (AWGN) channel uses. The set of all possible codewords \mathbf{x} is a nonbinary code of length N . As the mapping Φ is one-to-one, an alternative binary code \mathcal{C} of length mN can be constructed. Assuming the information messages to be equiprobable, the rate of the binary code is $R_C = \log_2(|\mathcal{C}|)/(mN)$. At the transmitter, a binary codeword $\mathbf{b} \in \mathcal{C}$ is selected and at the receiver a length- mN vector of L-values \mathbf{l} is calculated. With a slight abuse of notation, we write $b_{j,i}$ and $l_{j,i}$ to denote the j th input bit to the modulator and the j th L-value from the demapper in the i th channel use, respectively. In the length- mN vector \mathbf{b} (and similarly for \mathbf{l}) $b_{j,i}$ corresponds to the entry $b_{N(j-1)+i}$. This way, all input bits that correspond to a particular bit position appear consecutively in \mathbf{b} , i.e., $\mathbf{b} = [\dots, b_{j,1}, b_{j,2}, \dots, b_{j,N}, b_{j+1,1}, \dots]$.

The standard BICM decoder we consider in this paper is defined as [6]

$$\hat{\mathbf{b}} = \underset{\mathbf{b} \in \mathcal{C}}{\operatorname{argmax}} \sum_{i=1}^N \sum_{j=1}^m b_{j,i} l_{j,i} \quad (5)$$

i.e., the decoder finds the codeword that maximizes the correlation with the vector of the observed L-values. The codeword error probability is defined as $P_e = \Pr\{\hat{\mathbf{B}} \neq \mathbf{B}\}$.

To simplify the notation, one of the indices i, j may be omitted depending on the discussed context. To avoid ambiguity, in the remaining of the paper, the following convention applies: the index $1 \leq j \leq m$ is used to indicate the bit position and the index $1 \leq i \leq N$ is used to indicate the time instant.

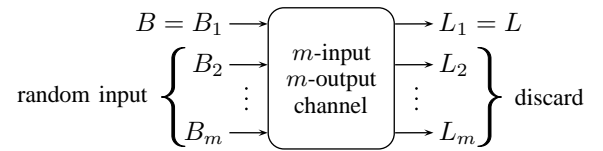


Fig. 4: Bit-level channel, illustrated for the first bit position.

III. BIT-LEVEL ANALYSIS

When analyzing achievable rates of BICM, it is common to proceed with a parallel independent channel model and assume that there exist m independent bit channels from B_j to L_j . This assumption is typically motivated by the insertion of the so-called “ideal interleaver” [5, Sec. II-B]. In this paper, we use a different approach which does not rely on any interleaver or independence assumption between bit channels. We reduce the m -input m -output channel in Fig. 1 to a channel with only one binary input and one continuous output. This can be done by specifying a behavioral model for the other, unused bit positions. To that end, consider the hypothetical scenario where we are only interested in transmitting data from B_j to L_j . To do so, we may feed the modulator at all other bit positions $j' \neq j$ with independent and uniformly distributed (i.u.d.) bits. At the receiver side, we discard all L-values except the one of interest. This is conceptually shown in Fig. 4 for $j = 1$ leading to a binary-input, continuous-output channel from B_1 to L_1 .

Since the results in this section are not dependent on any particular j , the bit-level index j is dropped. Definitions and equations that hold for both exact and max-log L-values will be stated with the generic placeholder variable L . As an example, the generic bit-level channel in Fig. 4 is denoted by $f_{L|B}(\cdot|\cdot)$. For exact L-values, the channel is then denoted by $f_{L^{\text{ex}}|B}(\cdot|\cdot)$. Note that this conditional PDF is hard to calculate in general [17, Ch. 4]. For max-log L-values, the channel is denoted by $f_{L^{\text{ml}}|B}(\cdot|\cdot)$. This conditional PDF is relatively easy to obtain due to the special form of (4) and corresponds to a summation of piecewise Gaussian functions (see [11] and references therein).

A. Bit-Level Coding Scheme

The coding scheme for the bit-level channel in Fig. 4 is obtained from the one described in Sec. II-D by simply omitting irrelevant bit positions. Let $\mathcal{C} \subset \{0, 1\}^N$ denote a binary code of length N and rate $R = \log_2(|\mathcal{C}|)/N$. The decoder in (5) then reduces to

$$\hat{\mathbf{b}} = \underset{\mathbf{b} \in \mathcal{C}}{\operatorname{argmax}} \sum_{i=1}^N b_i l_i \quad (6)$$

where the l_i are either exact or max-log L-values.

B. Achievable Rates

1) *Generalized Mutual Information:* It has been shown in [18] that for the decoder in (6), the maximum achievable rate is lowerbounded by (cf. [8, eq. (18)])

$$\text{GMI}_L = 1 - \inf_{s \geq 0} \mathbb{E} \left\{ \log_2 \left(1 + e^{-s \hat{B} L} \right) \right\}. \quad (7)$$

We refer to this quantity as the bit-level GMI or simply GMI. The GMI has the following operational meaning. There exists a binary code \mathcal{C} with rate arbitrarily close to GMI_L that can achieve reliable communication (i.e., $P_e < \varepsilon$ for ε as small as desired) as $N \rightarrow \infty$ over the channel from B to L assuming the decoder in (6). The codewords of such a code \mathcal{C} are composed of i.u.d. bits [18]. We will use this fact later on when discussing the BICM GMI.

2) *Mutual Information*: Lifting the decoder assumption, an achievable rate for the channel in Fig. 4 is given by the MI between B and L defined as [19, p. 251]

$$\text{MI}_L = I(B; L) = \mathbb{E} \left\{ \log_2 \left(\frac{f_{L|B}(L|B)}{f_L(L)} \right) \right\}. \quad (8)$$

The MI has a similar operational meaning as the GMI, but does not make any restrictions regarding the decoder structure. In particular, for the channel from B to L , there exists a binary code \mathcal{C} with rate arbitrarily close to MI_L that can achieve reliable communication as $N \rightarrow \infty$. Furthermore, the MI is the *maximum* achievable rate. Note that both the GMI and the MI are functions of the SNR. However, to simplify the notation, we omitted the dependence on ρ .

The following lemma is the main reason why only symmetric constellations are considered in the paper.

Lemma 1. *For symmetric M -PAM constellations, equivalent patterns give the same GMI and MI.*

Proof: Using (3)–(4) one can show that the L-value $l(y)$ for a pattern \mathbf{p} and the L-value $l'(y)$ for the reflected pattern $\mathbf{p}' = \text{refl}(\mathbf{p})$ are related by $l(y) = l'(-y)$. Similarly, the L-values for a pattern and the inverted pattern are related by $l(y) = -l'(y)$. It follows from (7)–(8) that inverting and/or reflecting a pattern does not affect the corresponding GMI and MI. \square

C. L-values

1) *Exact L-values*: For exact L-values, the decoder (6) corresponds to the maximum likelihood decoder for the channel $f_{L^{\text{ex}}|B}(\cdot|\cdot)$. This explains that for exact L-values, the GMI is equivalent to the MI. In fact, the MI for exact L-values can alternatively be written as

$$\text{MI}_{L^{\text{ex}}} = I(B; L^{\text{ex}}) = I(B; Y) = \text{GMI}_{L^{\text{ex}}} \quad (9)$$

and the infimum in (7) is achieved for $s = 1$, as shown in [6, Corollary 1].

2) *Max-Log L-values*: For max-log L-values, the MI is given by

$$\text{MI}_{L^{\text{ml}}} = I(B; L^{\text{ml}}). \quad (10)$$

Unlike for exact L-values, $\text{MI}_{L^{\text{ml}}} \geq \text{GMI}_{L^{\text{ml}}}$. This is because max-log L-values are not true log-likelihood ratios for the channel $f_{L^{\text{ml}}|B}(\cdot|\cdot)$ and hence, the decoder in (6) does not correspond to a maximum likelihood decoder. However, applying different functions to L^{ml} may increase the corresponding GMI, which is in sharp contrast to the MI and the data

processing inequality [19, Theorem 2.8.1]. In [7, Theorem 1], it is shown that $\text{MI}_{L^{\text{ml}}} = \text{GMI}_{g(L^{\text{ml}})}$ for

$$g(l) = \log \left(\frac{f_{L^{\text{ml}}|B}(l|1)}{f_{L^{\text{ml}}|B}(l|0)} \right). \quad (11)$$

The intuitive interpretation is that the processing in (11) matches the metrics to the decoder (6), and hence, makes the decoder a maximum likelihood decoder.

We can compare the discussed achievable rates in the form of the following chain of inequalities

$$\text{GMI}_{L^{\text{ex}}} = \text{MI}_{L^{\text{ex}}} \stackrel{(a)}{\geq} \text{MI}_{L^{\text{ml}}} = \text{GMI}_{g(L^{\text{ml}})} \geq \text{GMI}_{L^{\text{ml}}} \quad (12)$$

where inequality (a) follows from the data processing inequality. As mentioned in Sec. I, it is commonly assumed that inequality (a) is strict. In the next section, we show that this inequality is in fact an equality in some cases.

D. Lossless Patterns

We start with the following lemma.

Lemma 2. *For any one-dimensional constellation and any pattern, $\text{MI}_{L^{\text{ex}}} = \text{MI}_{L^{\text{ml}}}$ if and only if there exist a function $f(\cdot)$ such that $L^{\text{ex}} = f(L^{\text{ml}})$.*

Proof: The “if” part follows from the data processing inequality. The “only if” follows from the fact that exact L-values form a *minimal* sufficient statistic for guessing B based on Y . In particular, assume $L^{\text{ml}}(y) = L^{\text{ml}}(y')$ for two channel observations y and y' . If $\text{MI}_{L^{\text{ml}}} = \text{MI}_{L^{\text{ex}}}$ (and hence max-log L-values also form a sufficient statistic), it follows from Fisher’s factorization theorem [20, Ch. 22.3] that $f_{Y|B}(y|b)/f_{Y|B}(y'|b)$ is independent of b , which implies $L^{\text{ex}}(y) = L^{\text{ex}}(y')$. Thus, there has to exist a one-to-one mapping between L^{ex} and L^{ml} . \square

Based on this lemma, we have the following theorem.

Theorem 1. *For symmetric M -PAM constellations and all patterns equivalent to $\mathbf{p}_1 = [\mathbf{0}_{M/2}, \mathbf{1}_{M/2}]$ and $\mathbf{p}_2 = [\mathbf{0}_{M/4}, \mathbf{1}_{M/2}, \mathbf{0}_{M/4}]$, the max-log approximation does not induce any information loss, i.e., $\text{MI}_{L^{\text{ex}}} = \text{MI}_{L^{\text{ml}}}$. For all other patterns, $\text{MI}_{L^{\text{ex}}} > \text{MI}_{L^{\text{ml}}}$.*

Proof: The proof is given in Appendix A. \square

As an example, for 4-PAM, there exist only three patterns that are not equivalent, i.e., $\mathbf{p}_1 = [0, 0, 1, 1]$, $\mathbf{p}_2 = [0, 1, 1, 0]$, and $\mathbf{p}_3 = [0, 1, 0, 1]$. The first two patterns are lossless according to Theorem 1 and they correspond to the first and the second bit position in the BRGC, respectively. For the NBC, the first and second bit positions correspond to the patterns \mathbf{p}_1 and \mathbf{p}_3 , respectively (see Fig. 2). From Theorem 1, the first bit position is again information lossless while the second one is not. In fact, we immediately have the following corollary.

Corollary 1. *Among all possible combinations of symmetric M -PAM constellations and labelings, 4-PAM with the BRGC (or any equivalent labeling) is the only case where all bit positions are information lossless.*

Proof: It is easy to show that \mathbf{p}_1 and \mathbf{p}_2 or their equivalent patterns cannot be used twice in a labeling. This means that

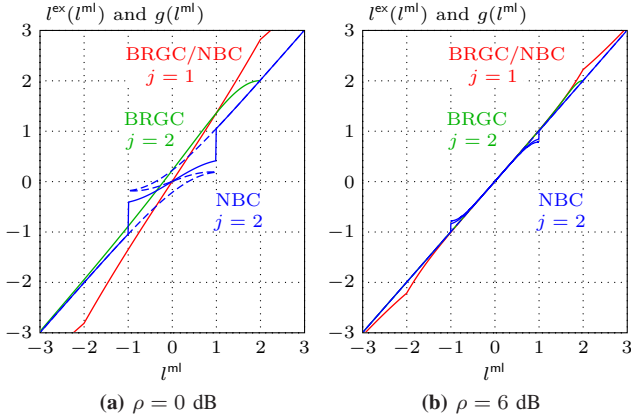


Fig. 5: The correction function $g(\cdot)$ (solid) and the exact L-value versus the max-log L-value (dashed) for the three non-equivalent patterns for an equally spaced 4-PAM constellation. The values on the x- and y-axes are normalized by $4\rho/5$.

any labeling with more than two bit positions will contain a bit pattern for which the max-log approximation causes an information loss. \square

It is interesting to look at the function (11) and compare it with the curve obtained by plotting l^{ex} versus l^{ml} , as shown in Fig. 5 for the three non-equivalent patterns p_1 (red), p_2 (green), and p_3 (blue). In general, for the lossless patterns, this function coincides with the curve l^{ex} versus l^{ml} and for lossy patterns it does not. The information loss then comes from the region where $g(\cdot)$ cannot recover the exact L-value.

IV. BICM ANALYSIS

In this section, we return from the bit-level viewpoint to the original m -input m -output channel shown in Fig. 1. The results presented in this section are not constellation-specific and hold for any one-dimensional constellation with 2^m points, where $m > 2$.

A. BICM Mutual Information

The BICM MI is defined as

$$\text{MI}_{\mathbf{L}}^{\text{bicm}} = \sum_{j=1}^m \text{MI}_{L_j} = \sum_{j=1}^m I(B_j; L_j) \quad (13)$$

i.e., the sum of m bit-level MIs, for both exact (cf. [5, eq. (15)]) and max-log L-values. Under the parallel independent channel model assumption [5], it is the maximum achievable rate for exact L-values with the standard BICM decoder (5). However, in the case of the model in Fig. 1, its operational meaning as an upper bound on the achievable rate is unclear. Using the mismatched decoding framework, it was shown to be an achievable rate for the standard BICM decoder [6, Sec. III]. It is also achievable for max-log L-values, provided that the ideal correction function $g(\cdot)$ is applied for each bit level before decoding via (5).

B. BICM Generalized Mutual Information

The BICM GMI is defined as [6, eq. (59)]

$$\text{GMI}_{\mathbf{L}}^{\text{bicm}} = m - \inf_{s \geq 0} \sum_{j=1}^m \mathbb{E} \left\{ \log_2 \left(1 + e^{-s \tilde{B}_j L_j} \right) \right\} \quad (14)$$

and was shown to be an achievable rate for the decoder in (5) [6, Sec. III]. For exact L-values, similarly to the bit-level GMI in (7) (see also (9)), the value $s = 1$ maximizes the BICM GMI in (14). In that case, the BICM GMI can be written as a sum of bit-level GMIs. This, however, does not hold for max-log L-values.

It has recently been shown in [8] that the so-called ‘‘harmonized’’ GMI defined as

$$\begin{aligned} \text{GMI}_{\mathbf{L}}^{\text{harm}} &= \sum_{j=1}^m \text{GMI}_{L_j} \\ &= m - \sum_{j=1}^m \inf_{s_j \geq 0} \mathbb{E} \left\{ \log_2 \left(1 + e^{-s_j \tilde{B}_j L_j} \right) \right\} \end{aligned} \quad (15)$$

is achievable when max-log L-values are used and different linear corrections are applied to L-values at different bit levels. Note that, unlike the BICM GMI, the harmonized GMI in (15) corresponds to the sum of m bit-level GMIs for both exact and max-log L-values. By exploiting the bit-level viewpoint in Sec. III, we show in the following theorem that the harmonized GMI is achievable by the standard BICM decoder without the assumption of any L-value correction.

Theorem 2. *For any one-dimensional constellation and any labeling, the rate $\text{GMI}_{\mathbf{L}}^{\text{harm}}$ in (15) is achievable by the standard BICM decoder (5).*

Proof: We know from Sec. III-A that for each bit level, there exists a binary code \mathcal{C}_j of length N with rate close to GMI_{L_j} achieving reliable communication for the decoder

$$\hat{\mathbf{b}}_j = \underset{\mathbf{b} \in \mathcal{C}_j}{\text{argmax}} \sum_{i=1}^N b_i l_{j,i} \quad (16)$$

under the assumption that we feed i.u.d. bits to the other bit positions. The binary code \mathcal{C}_j itself consists of codewords with i.u.d. bits.

If we now consider the code $\mathcal{C} = \mathcal{C}_1 \times \dots \times \mathcal{C}_m$ of length mN , where each codeword in \mathcal{C} is a concatenation of codewords in $\mathcal{C}_1, \dots, \mathcal{C}_m$, the decoding rule (5) can be decomposed as

$$\max_{\mathbf{b} \in \mathcal{C}} \sum_{i=1}^N \sum_{j=1}^m b_{j,i} l_{j,i} = \sum_{j=1}^m \left(\max_{\mathbf{b} \in \mathcal{C}_j} \sum_{i=1}^N b_i l_{j,i} \right). \quad (17)$$

Hence, the decoder is given by

$$\begin{aligned} \hat{\mathbf{b}} &= \left[\underset{\mathbf{b} \in \mathcal{C}_1}{\text{argmax}} \sum_{i=1}^N b_i l_{1,i}, \dots, \underset{\mathbf{b} \in \mathcal{C}_m}{\text{argmax}} \sum_{i=1}^N b_i l_{m,i} \right] \\ &= [\hat{\mathbf{b}}_1, \dots, \hat{\mathbf{b}}_m]. \end{aligned} \quad (18)$$

The code construction guarantees that coded bits across different bit positions are independent. Since each code \mathcal{C}_j fulfils the requirement on the input distribution (i.e., the coded bits

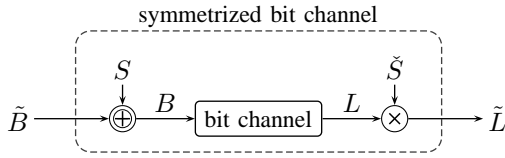


Fig. 6: Illustration of the channel symmetrization technique via i.i.d. bit adapters. S is assumed to be known by both the transmitter and receiver and added to B modulo 2 at the transmitter.

are uniform), the probability that a subcodeword is incorrect is $\Pr\{\hat{\mathbf{B}}_j \neq \mathbf{B}_j\} < \varepsilon_j$. In this case, the overall error probability is bounded by $P_e < \sum_{j=1}^m \varepsilon_j$, and thus, the probability of error can be made arbitrarily small. \square

C. Inequalities

To clarify the difference between the achievable rates for exact and max-log L-values discussed in this section, we give a short summary in the form of the following inequalities. For exact L-values, all studied quantities are the same and we have

$$\text{MI}_{L^{\text{ex}}}^{\text{bicm}} = \text{GMI}_{L^{\text{ex}}}^{\text{harm}} = \text{GMI}_{L^{\text{ex}}}^{\text{bicm}} \quad (20)$$

which is the rate that is achievable by the standard BICM decoder.

The value in (20) is an upper bound on the corresponding quantities for max-log L-values, i.e.,

$$\text{MI}_{L^{\text{ex}}}^{\text{bicm}} \geq \text{MI}_{L^{\text{ml}}}^{\text{bicm}} \geq \text{GMI}_{L^{\text{ml}}}^{\text{harm}} \geq \text{GMI}_{L^{\text{ml}}}^{\text{bicm}}. \quad (21)$$

As previously mentioned, the second quantity is an achievable rate if the function (11) is applied to the max-log L-values from the m different bit positions before passing them to the decoder (5). The third quantity is a rate achievable by the standard BICM decoder (5) without any L-value correction. The last quantity corresponds to the BICM GMI as defined in [6, eq. (59)] for max-log L-values. As shown in Corollary 1, the first inequality is an equality only for 4-PAM labeled with a binary labeling equivalent to the BRGC.

V. L-VALUE PROCESSING

A. Symmetrization

In this subsection, we study how bit-level channel symmetrization affects the GMI and the MI for exact and max-log L-values. Bit-level symmetrization can be motivated as follows. A binary input channel $f_{L|B}(\cdot|\cdot)$ is said to be output symmetric if

$$f_{L|B}(l|b) = f_{L|B}(-l|\bar{b}). \quad (22)$$

For some patterns, for instance for $\mathbf{p} = [0, 1, 1, 0]$, the channel is not output symmetric (neither for exact nor max-log L-values), which complicates the analysis of BICM systems in certain cases. For example, one cannot assume the transmission of the all-zero codeword when studying the error probability P_e of a linear code over such a channel.

To enforce an output symmetric channel, it was proposed in [5] to use a randomly complemented labeling. In [21], a similar symmetrization technique was realized by the use of

random independent identically distributed (i.i.d.) bit adapters as shown in Fig. 6. At the transmitter, a uniformly random bit S is added modulo 2 to the transmitted bit and at the receiver, the L-value is multiplied by $\check{S} = (-1)^S$. This implies that S is known to both the transmitter and the receiver. However, S is not known to the decoder, and hence, the adapter is considered part of the channel¹. If we denote the symmetrized L-value by \tilde{L} , the conditional PDF of \tilde{L} can be related to the conditional PDF of the original L-value through

$$f_{\tilde{L}|\tilde{B}}(l|b) = \frac{1}{2} (f_{L|B}(l|b) + f_{L|B}(-l|\bar{b})). \quad (23)$$

In [21, Theorem 2], it was shown that the MI is unchanged by the symmetrization if exact L-values are used. Somewhat surprisingly, the effect of this operation on the MI and the GMI for max-log L-values has not been studied in the literature. In the following, we show that the GMI is not affected by the symmetrization, while the MI is reduced for max-log L-values.

Theorem 3. *For any one-dimensional constellation and any pattern, the bit-level channel symmetrization does not change the GMI in (7), i.e.,*

$$\text{GMI}_{\tilde{L}} = \text{GMI}_L. \quad (24)$$

Proof: Let $h(x) = \log_2(1 + e^{-x})$. The expectation in (7) with respect to \tilde{L} can then be written as

$$\mathbb{E} \left\{ h(s\check{B}\tilde{L}) \right\} \quad (25)$$

$$= \frac{1}{2} \sum_{b \in \mathcal{B}} \int_{-\infty}^{\infty} f_{\tilde{L}|\tilde{B}}(l|b) h(s\check{b}l) dl \quad (26)$$

$$\stackrel{(23)}{=} \frac{1}{4} \sum_{b \in \mathcal{B}} \int_{-\infty}^{\infty} (f_{L|B}(l|b) + f_{L|B}(-l|\bar{b})) h(s\check{b}l) dl \quad (27)$$

$$= \frac{1}{2} \sum_{b \in \mathcal{B}} \int_{-\infty}^{\infty} f_{L|B}(l|b) h(s\check{b}l) dl \quad (28)$$

$$= \mathbb{E} \left\{ h(s\check{B}L) \right\}. \quad (29)$$

\square

Intuitively, this result can be explained by the fact that the decoder (6) does not exploit the information about the asymmetry of the L-values even if it is available.

Corollary 2. *For exact L-values, $\text{MI}_{\tilde{L}^{\text{ex}}} = \text{MI}_{L^{\text{ex}}}$.*

Proof: The result was already proved in [21, Theorem 2]. It also follows directly from Theorem 3 using the equivalence of the GMI and the MI for exact L-values in (9).² \square

Corollary 3. *For max-log L-values, $\text{MI}_{\tilde{L}^{\text{ml}}} \leq \text{MI}_{L^{\text{ml}}}$.*

The proof follows directly from the data processing inequality. Corollary 3 can be interpreted in the following way. In order to achieve $\text{MI}_{L^{\text{ml}}}$, the correction function $g(\cdot)$ in (11) needs to be applied to the L-values prior to decoding (6). Hence, the information about the asymmetry of the L-values

¹The considered system model is equivalent to the one in Sec. III if S is known to the decoder.

²As pointed out in [21, Theorem 2], after symmetrization we lose an opportunity to optimize the input distribution, and therefore, the symmetrization may decrease the channel capacity. Channel capacity, however, is not studied in this paper.

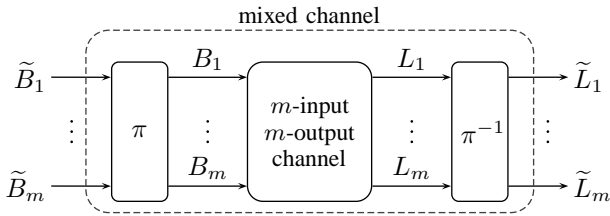


Fig. 7: Block diagram showing the mixing of bit positions. The interleaver π reorders the bit levels.

is exploited by means of $g(\cdot)$. This information might not be available after the symmetrization, which causes the decrease of the mutual information. From this analysis and Theorem 1, we conclude that the losses observed in [11, Fig. 4] and [12, Fig. 2] come partly from the L-value symmetrization for constellations larger than 16-ary QAM, whereas the loss for 16-QAM is solely due to the symmetrization and not due to the max-log approximation. This is in contrast to the discussion included in [11], [12], where the loss is attributed solely to the max-log approximation.

B. Channel Mixing

Channel mixing is another popular operation that is often assumed in order to simplify the analysis of BICM systems [22]. Channel mixing can be visualized in Fig. 7, where in addition to the m -input m -output channel, an interleaver π and a deinterleaver π^{-1} are introduced. The interleaver randomly and uniformly assigns the input bits to the channel inputs and the deinterleaver performs the reverse operation. Similarly to the previous section, the random assignments of the bits are known to the transmitter and the receiver. However, they are unknown to the decoder. For mixed channels, the m L-values $\tilde{L}_1, \dots, \tilde{L}_m$ from different bit positions have the same distribution and hence can be treated equally, where the PDF is given by

$$f_{\tilde{L}|\tilde{B}}(l|b) = \frac{1}{m} \sum_{j=1}^m f_{L_j|B_j}(l|b). \quad (30)$$

It is often said that channel mixing does not increase the BICM MI, cf. [22, Theorem 2], which is obvious from the data processing inequality. In the following, we show that channel mixing does not reduce the BICM GMI either. As in the case of the bit-level symmetrization, the effect on the BICM MI depends on whether exact or max-log L-values are used.

Theorem 4. *For any one-dimensional constellation and any labeling, channel mixing does not affect the BICM GMI. In fact, we have*

$$\text{GMI}_{\tilde{L}}^{\text{harm}} = \text{GMI}_{\tilde{L}}^{\text{bicm}} = \text{GMI}_{\tilde{L}}^{\text{bicm}}. \quad (31)$$

Proof: Using the definition of the harmonized GMI in (15) and the fact that the mixed L-values all have the same

distribution we can write

$$\begin{aligned} \text{GMI}_{\tilde{L}}^{\text{harm}} &= m - \sum_{j=1}^m \inf_{s_j > 0} \mathbb{E} \left\{ \log \left(1 + e^{-s_j \tilde{B}_j \tilde{L}_j} \right) \right\} \\ &= m - \inf_{s_1 > 0} \sum_{j=1}^m \mathbb{E} \left\{ \log \left(1 + e^{-s_1 \tilde{B}_j \tilde{L}_j} \right) \right\} \quad (32) \end{aligned}$$

$$\begin{aligned} &= m - \inf_{s_1 > 0} \frac{m}{2} \sum_{b \in \mathcal{B}} \int_{-\infty}^{\infty} f_{\tilde{L}_1|\tilde{B}_1}(l|b) \log \left(1 + e^{-s_1 \tilde{b} l} \right) dl \\ &\stackrel{(30)}{=} m - \inf_{s_1 > 0} \frac{1}{2} \sum_{b \in \mathcal{B}} \int_{-\infty}^{\infty} \sum_{j=1}^m f_{L_j|B_j}(l|b) \log \left(1 + e^{-s_1 \tilde{b} l} \right) dl \\ &= m - \inf_{s_1 > 0} \sum_{j=1}^m \frac{1}{2} \sum_{b \in \mathcal{B}} \int_{-\infty}^{\infty} f_{L_j|B_j}(l|b) \log \left(1 + e^{-s_1 \tilde{b} l} \right) dl \\ &= m - \inf_{s_1 > 0} \sum_{j=1}^m \mathbb{E} \left\{ \log \left(1 + e^{-s_1 \tilde{B}_j \tilde{L}_j} \right) \right\} \quad (33) \end{aligned}$$

where (32) proves the first equality in (31) and (33) proves the second equality. \square

Although channel mixing does not affect the BICM GMI, it may reduce the harmonized GMI for max-log L-values, i.e., $\text{GMI}_{\tilde{L}^{\text{ml}}}^{\text{harm}} \leq \text{GMI}_{\tilde{L}^{\text{ml}}}^{\text{harm}}$. Using the result of Theorem 4 and (20) we conclude the following.

Corollary 4. *For exact L-values, $\text{MI}_{\tilde{L}^{\text{ex}}}^{\text{bicm}} = \text{MI}_{\tilde{L}^{\text{ex}}}^{\text{bicm}}$.*

This means that channel mixing does not decrease the MI for exact L-values, which justifies the use of this operation for the MI analysis. However, this is not the case when max-log L-values are used. The data processing inequality gives the following corollary.

Corollary 5. *For max-log L-values, $\text{MI}_{\tilde{L}^{\text{ml}}}^{\text{bicm}} \leq \text{MI}_{\tilde{L}^{\text{ml}}}^{\text{bicm}}$.*

The numerical results illustrating this inequality are provided in the next section.

VI. NUMERICAL EXAMPLES

We first present numerical examples for the bit-level analysis to illustrate the inequalities in (12). We consider the equally spaced 4-PAM constellation with the three nonequivalent patterns defined in Sec. III-D. Fig. 8 shows the loss in dB for different achievable rates in (12) with respect to (w.r.t.) $\text{MI}_{L^{\text{ex}}}$ as a function of the information rate in bits per channel use (bpcu). The solid lines show the loss for the $\text{GMI}_{L^{\text{ml}}}$. It can be seen that the GMI for max-log L-values is always inferior to the MI for exact L-values. An interesting behavior of the GMI for the pattern p_2 at asymptotically low SNR is that the loss grows unboundedly when the rate goes to zero (or equivalently, when the SNR tends to zero).

The dashed line in Fig. 8 shows the loss for $\text{MI}_{L^{\text{ml}}}$. There is only one dashed line in the figure as two of the three patterns are information lossless. Finally, the dash-dotted line illustrates the effect of the symmetrization on the MI and confirms Corollary 3.

As for the BICM analysis, we consider an equally spaced 4-PAM constellation labeled with the NBC. Fig. 9 shows the loss for different achievable rates w.r.t. to the $\text{MI}_{L^{\text{ex}}}^{\text{bicm}}$ as a function

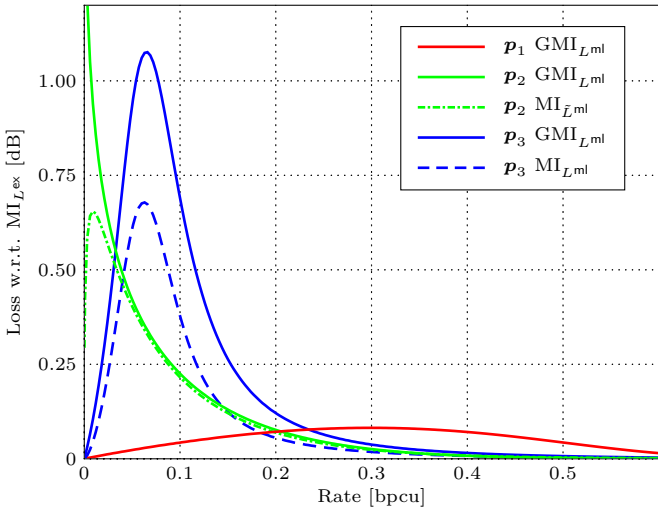


Fig. 8: Different losses for the three patterns for an equally spaced 4-PAM constellation.

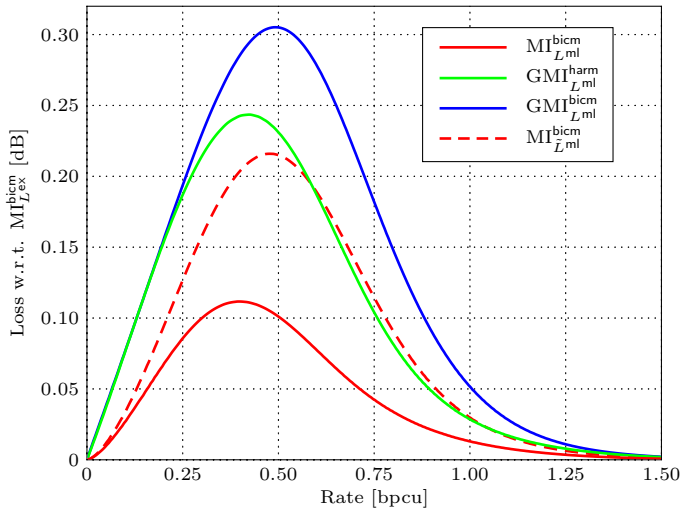


Fig. 9: Different achievable rates for 4-PAM with the NBC.

of the information rate. We note that the third inequality in (21) becomes an equality, i.e., $\text{GMI}_{L^{\text{ml}}}^{\text{harm}} = \text{GMI}_{L^{\text{ml}}}^{\text{bim}}$, for $R \approx 0.137$. The solid lines illustrate the inequalities (21), whereas the dashed line shows the effect of channel mixing formulated in Corollary 5.

Based on the presented results, we conclude that the losses due to the max-log approximation are in general small and occur at low rates.

VII. CONCLUSION

In this paper, we studied achievable rates for a BICM system considering both exact and max-log L-values. It was shown that the max-log approximation is not an information lossy operation in some cases. Furthermore, when exact L-values are considered, seemingly different quantities, e.g., BICM MI, BICM GMI, or harmonized GMI, all lead to the same achievable rates. However, this is not the case for max-log L-values, i.e., the different quantities may give different achievable rates in general. From a practical perspective, the

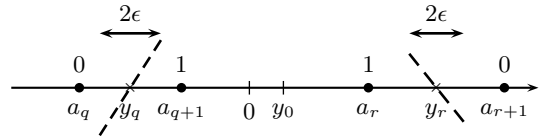


Fig. 10: Schematic representation of two zero-crossings for the max-log L-value $l^{\text{ml}}(y)$ (indicated with dashed lines).

difference between these quantities is rather small, especially for high SNR.

APPENDIX A PROOF OF THEOREM 1

We start by showing that for patterns \mathbf{p}_1 and \mathbf{p}_2 , the max-log approximation does not cause any information loss. Consider the pattern $\mathbf{p}_1 = [\mathbf{0}_{M/2}, \mathbf{1}_{M/2}]$ and the max-log L-value $l^{\text{ml}}(y)$ in (4). For a certain value y , let $a_q = \text{argmin}_{a \in \mathcal{S}_{j,0}} (y - a)^2$ and $a_r = \text{argmin}_{a \in \mathcal{S}_{j,1}} (y - a)^2$. The max-log L-value can then be written as $l^{\text{ml}}(y) = 2\rho(a_r - a_q)y + \rho(a_q^2 - a_r^2)$. Due to the structure of the pattern, $a_r > a_q$ for any value of y , which implies that its derivative $dl^{\text{ml}}(y)/dy$ is positive whenever it exists. This together with the fact that the L-value is a continuous function of the observation guarantees that $l^{\text{ml}}(y)$ is a monotonically increasing function. Therefore, $l^{\text{ml}}(y)$ is invertible, i.e., y can be recovered from $l^{\text{ml}}(y)$, and the exact L-value can be obtained from the max-log L-value.

Consider the pattern $\mathbf{p}_2 = [\mathbf{0}_{M/4}, \mathbf{1}_{M/2}, \mathbf{0}_{M/4}]$. From the structure of the pattern, it follows that $p_i = p_{M+1-i}$, i.e., the pattern is symmetric. It is therefore straightforward to show that $l^{\text{ex}}(y)$ and $l^{\text{ml}}(y)$ are even functions, i.e., $l^{\text{ex}}(y) = l^{\text{ex}}(|y|)$ and $l^{\text{ml}}(y) = l^{\text{ml}}(|y|)$. Thus, it is enough to show that $|y|$ is recoverable from $l^{\text{ml}}(y)$. This can be done by showing that $l^{\text{ml}}(y)$ is a decreasing function for $y \geq 0$, similarly to the first considered pattern.

$l^{\text{ml}}(y)$ has zero-crossings at midpoints between adjacent constellation points labeled with different bits. The pattern $\mathbf{p}_1 = [\mathbf{0}_{M/2}, \mathbf{1}_{M/2}]$ is the only pattern for which $l^{\text{ml}}(y)$ has exactly one zero-crossing and this pattern is lossless. In the following, we show that $\mathbf{p}_2 = [\mathbf{0}_{M/4}, \mathbf{1}_{M/2}, \mathbf{0}_{M/4}]$ is the only possible lossless pattern if $l^{\text{ml}}(y)$ has more than one zero-crossing.

Let y_q and y_r denote any two neighboring zero-crossings situated between the constellation points a_q and a_{q+1} , and a_r and a_{r+1} , respectively. This implies that $p_q = p_{r+1} = \bar{p}_{q+1} = \bar{p}_r$. Without loss of generality, we assume $p_q = 0$. Let $y_0 = (y_q + y_r)/2$ and without loss of generality we assume $y_0 \geq 0$. This is illustrated in Fig. 10.

The max-log L-value in (4) is a continuous piecewise linear function, where the slope of the pieces changes at the midpoints between neighboring constellation points labeled with the same bit. Since all constellation points are distinct, the slope of the max-log L-value cannot change at the zero-crossing, i.e., there exists an $\epsilon > 0$ such that

$$l^{\text{ml}}(y) = 2\rho(a_{q+1} - a_q)(y - y_q) \quad \text{for } y \in [y_q - \epsilon, y_q + \epsilon] \quad (34)$$

and

$$l^{\text{ml}}(y) = 2\rho(a_{r+1} - a_r)(y_r - y) \quad \text{for } y \in [y_r - \epsilon, y_r + \epsilon]. \quad (35)$$

The linear functions in (34)–(35) are shown with dashed lines in Fig. 10. Basically, ϵ indicates that there are nonzero intervals of y for which $l^{\text{ml}}(y)$ is a linear function that crosses the zero-level. One can then identify the values of y that give the same value of $l^{\text{ml}}(y)$. Based on (34)–(35), we can show that

$$l^{\text{ml}}(y + y_0) = l^{\text{ml}}(-\beta y + (2 - \beta)y_0 + (\beta - 1)y_r) \quad \text{for } y \in [y_r - y_0 - \epsilon, y_r - y_0 + \epsilon] \quad (36)$$

where

$$\beta = \frac{a_{r+1} - a_r}{a_{q+1} - a_q}. \quad (37)$$

In the following, we show that β has to equal one.

According to Lemma 2, for the max-log approximation to be information lossless, the exact L-value should be recoverable from the max-log L-value, i.e., the exact L-value should satisfy the condition

$$l^{\text{ex}}(y + y_0) = l^{\text{ex}}(-\beta y + (\beta - k)y_0 + (\beta - 1)y_r) \quad \text{for } y \in [y_r - y_0 - \epsilon, y_r - y_0 + \epsilon]. \quad (38)$$

If this condition is not satisfied, several values of $l^{\text{ex}}(y)$ will correspond to one value of $l^{\text{ml}}(y)$.

The nominator and the denominator of the exact L-value in (3) are sums of exponential functions and therefore, they are analytic functions, as is their ratio. The logarithm of an analytic function is analytic and hence the exact L-value is an analytic function. The condition (38) can be rewritten as

$$v(y) = 0, \quad \text{for } y \in [y_r - y_0 - \epsilon, y_r - y_0 + \epsilon] \quad (39)$$

where $v(y) = l^{\text{ex}}(y_0 - y) - l^{\text{ex}}(-\beta y + (2 - \beta)y_0 + (\beta - 1)y_r)$ is an analytic function. If an analytic function is zero on an interval, it has to be zero everywhere it is defined, i.e., $v(y) = 0$ for $y \in \mathbb{R}$ or

$$l^{\text{ex}}(y + y_0) = l^{\text{ex}}(-\beta y + (2 - \beta)y_0 + (\beta - 1)y_r) \quad \text{for } y \in \mathbb{R}. \quad (40)$$

Since $l^{\text{ex}}(y) \rightarrow l^{\text{ml}}(y) \forall y$ when $\rho \rightarrow \infty$, the same should hold for the max-log L-value, i.e.,

$$l^{\text{ml}}(y + y_0) = l^{\text{ml}}(-\beta y + (2 - \beta)y_0 + (\beta - 1)y_r) \quad \text{for } y \in \mathbb{R} \quad (41)$$

for $\rho \rightarrow \infty$. Since ρ appears as a scaling factor in (4), (41) in fact holds for any SNR values. The max-log L-value will then achieve the maximum value on the interval $[y_q, y_r]$ when the arguments of the right-hand side and the left-hand side in (41) are equal, i.e., at $y' = y'' + y_0$, where $y'' + y_0 = -\beta y'' + (2 - \beta)y_0 + (\beta - 1)y_r$. We can show that the maximum is achieved at

$$y' = y_0 + \frac{\beta - 1}{\beta + 1} \frac{y_r - y_q}{2}.$$

On the other hand, the maximum of the L-value should be at the midpoint between the constellation points a_q and a_{r+1} labeled with the zero bit since this is the point where the slope of the L-value in (4) changes its sign, i.e., $y' = (a_{r+1} +$

$a_q)/2 = y_0 + ((a_{r+1} - a_r) - (a_{q+1} - a_q))/4$. Therefore, the following should hold

$$\frac{\beta - 1}{\beta + 1} \frac{y_r - y_q}{2} = y_0 + \frac{(a_{r+1} - a_r) - (a_{q+1} - a_q)}{4}. \quad (42)$$

Using the definition of β in (37), one can easily show that (42) holds only for $\beta = 1$. We next show that y_0 has to equal zero to satisfy (41) for $\beta = 1$.

From (4) it follows that $\text{sign}(l^{\text{ml}}(y)) = (-1)^{\bar{p}_1}$ for $y < a_1$ and $\text{sign}(l^{\text{ml}}(y)) = (-1)^{\bar{p}_M}$ for $y > a_M$. Letting $y = a_1 - \gamma - y_0$ for some $\gamma > 0$ in (41) gives

$$l^{\text{ml}}(2y_0 - a_1 + \gamma) = l^{\text{ml}}(a_1 - \gamma). \quad (43)$$

Since $a_M = -a_1$, it is easy to see that $2y_0 - a_1 + \gamma > a_M$, hence $p_1 = p_M$. Without loss of generality, p_1 is assumed to be zero. Let $a_k = \text{argmin}_{a \in \mathcal{X}_1} (2y_0 - a_1 + \gamma - a)^2$ and $a_l = \text{argmin}_{a \in \mathcal{X}_1} (a_1 - \gamma - a)^2$, i.e., the points a_k and a_l are the outermost constellation points labeled with one from the right and from the left, respectively. Using the introduced notation, (43) can be rewritten as

$$(2y_0 - a_1 + \gamma - a_M)^2 - (2y_0 - a_1 + \gamma - a_k)^2 = (a_1 - \gamma - a_1)^2 - (a_1 - \gamma - a_l)^2 \quad (44)$$

which should hold for any $\gamma > 0$. Using $a_M = -a_1$, y_0 can be expressed as

$$y_0 = \frac{(a_k + a_l)(2a_1 + a_k - a_l - 2\gamma)}{4(a_1 + a_k)}. \quad (45)$$

By definition, y_0 is a constant and is independent of γ , which implies that $a_k = -a_l$ in (45) and $y_0 = 0$. This in turn means that for any two neighboring zero-crossings y_q and y_r , the midpoint $(y_q + y_r)/2$ has to be zero, i.e., only two zero-crossings are allowed for the pattern to be invertible. Therefore, an invertible pattern has to be of the form $\mathbf{p} = [\mathbf{0}_n, \mathbf{1}_{M/2}, \mathbf{0}_{M/2-n}]$ for $n = 1, \dots, M/2 - 1$. The only pattern of such a form that satisfies $a_k = -a_l$ is $\mathbf{p}_2 = [\mathbf{0}_{M/4}, \mathbf{1}_{M/2}, \mathbf{0}_{M/4}]$, which completes the proof.

REFERENCES

- [1] E. Zehavi, "8-PSK trellis codes for a Rayleigh channel," *IEEE Trans. Commun.*, vol. 40, no. 3, pp. 927–946, May 1992.
- [2] IEEE 802.11, "Part 11: Wireless LAN medium access control (MAC) and physical layer (PHY) specifications," IEEE Std 802.11-2012, Tech. Rep., Mar. 2012.
- [3] ETSI, "LTE; Evolved universal terrestrial radio access (E-UTRA); Physical channels and modulation," ETSI, Tech. Rep. ETSI TS 136 211 V11.2.0 (2013-04), Apr. 2013.
- [4] ETSI, "Digital video broadcasting (DVB); Frame structure channel coding and modulation for a second generation digital terrestrial television broadcasting system (DVB-T2)," ETSI, Tech. Rep. ETSI EN 302 755 V1.3.1 (2012-04), Apr. 2012.
- [5] G. Caire, G. Taricco, and E. Biglieri, "Bit-interleaved coded modulation," *IEEE Trans. Inf. Theory*, vol. 44, no. 3, pp. 927–946, May 1998.
- [6] A. Martinez, A. Guillén i Fàbregas, G. Caire, and F. Willems, "Bit-interleaved coded modulation revisited: A mismatched decoding perspective," *IEEE Trans. Inf. Theory*, vol. 55, no. 6, pp. 2756–2765, June 2009.
- [7] J. Jaldén, P. Fertl, and G. Matz, "On the generalized mutual information of BICM systems with approximate demodulation," in *Proc. IEEE Information Theory Workshop (ITW)*, Jan. 2010.
- [8] T. Nguyen and L. Lampe, "Bit-interleaved coded modulation with mismatched decoding metrics," *IEEE Trans. Commun.*, vol. 59, no. 2, pp. 437–447, Feb. 2011.

- [9] L. Szczecinski, "Correction of mismatched L-values in BICM receivers," *IEEE Trans. Commun.*, vol. 60, no. 11, pp. 3198–3208, Nov. 2012.
- [10] C. Stierstorfer, "A bit-level-based approach to coded multicarrier transmission," Ph.D. dissertation, Friedrich-Alexander-Universität Erlangen-Nürnberg, Erlangen, Germany, 2009, available at <http://www.opus.ub.uni-erlangen.de/opus/volltexte/2009/1395/>.
- [11] A. Alvarado, L. Szczecinski, R. Feick, and L. Ahumada, "Distribution of L-values in Gray-mapped M^2 -QAM: Closed-form approximations and applications," *IEEE Trans. Commun.*, vol. 57, no. 7, pp. 2071–2079, July 2009.
- [12] L. Szczecinski, A. Alvarado, and R. Feick, "Distribution of max-log metrics for QAM-based BICM in fading channels," *IEEE Trans. Commun.*, vol. 57, no. 9, pp. 2558–2563, Sep. 2009.
- [13] G. Ungerboeck, "Channel coding with multilevel/phase signals," *IEEE Trans. Inf. Theory*, vol. IT-28, no. 1, pp. 55–67, Jan. 1982.
- [14] M. Ivanov, F. Brännström, A. Alvarado, and E. Agrell, "On the exact BER of bit-wise demodulators for one-dimensional constellations," *IEEE Trans. Commun.*, vol. 61, no. 4, pp. 1450–1459, Apr. 2013.
- [15] E. Agrell, J. Lassing, E. G. Ström, and T. Ottosson, "On the optimality of the binary reflected Gray code," *IEEE Trans. Inf. Theory*, vol. 50, no. 12, pp. 3170–3182, Dec. 2004.
- [16] A. J. Viterbi, "An intuitive justification and a simplified implementation of the MAP decoder for convolutional codes," *IEEE J. Sel. Areas Commun.*, vol. 16, no. 2, pp. 260–264, Feb. 1998.
- [17] A. Guillén i Fàbregas, A. Martínez, and G. Caire, "Bit-interleaved coded modulation," *Foundations and Trends in Communications and Information Theory*, vol. 5, no. 1–2, pp. 1–153, 2008.
- [18] A. Ganti, A. Lapidath, and I. E. Telatar, "Mismatched decoding revisited: General alphabets, channels with memory, and the wide-band limit," *IEEE Trans. Inf. Theory*, vol. 46, no. 7, pp. 2315–2328, Nov. 2000.
- [19] T. M. Cover and J. A. Thomas, *Elements of information theory*, 2nd ed. Wiley-Interscience, 2006.
- [20] A. Lapidath, *A Foundation in Digital Communication*. Cambridge University Press, 2009.
- [21] J. Hou, P. H. Siegel, L. B. Milstein, and H. D. Pfister, "Capacity-approaching bandwidth-efficient coded modulation schemes based on low-density parity-check codes," *IEEE Trans. Inf. Theory*, vol. 49, no. 9, pp. 2141–2155, Sep. 2003.
- [22] Q. Xie, Z. Wang, and Z. Yang, "Simplified soft demapper for APSK with product constellation labeling," *IEEE Trans. Wireless Commun.*, vol. 11, no. 7, pp. 2649–2657, July 2012.